JCI insight

# A replication-competent late liver stage–attenuated human malaria parasite

Debashree Goswami, … , Ashley M. Vaughan, Stefan H.I. Kappe

*JCI Insight.* 2020;5(13):e135589. https://doi.org/10.1172/jci.insight.135589.

Research Article | Infectious disease | Vaccines

Whole-sporozoite vaccines engender sterilizing immunity against malaria in animal models and importantly, in humans. Gene editing allows for the removal of specific parasite genes, enabling generation of genetically attenuated parasite (GAP) strains for vaccination. Using rodent malaria parasites, we have previously shown that late liver stage–arresting replication-competent (LARC) GAPs confer superior protection when compared with early liver stage–arresting replication-deficient GAPs and radiation-attenuated sporozoites. However, generating a LARC GAP in the human malaria parasite *Plasmodium falciparum* (*P. falciparum*) has been challenging. Here, we report the generation and characterization of a likely unprecedented *P. falciparum* LARC GAP generated by targeted gene deletion of the *Mei2* gene: *P. falciparum mei2*$^{-}$. Robust exoerythrocytic schizogony with extensive cell growth and DNA replication was observed for *P. falciparum mei2*$^{-}$ liver stages in human liver-chimeric mice. However, *P. falciparum mei2*$^{-}$ liver stages failed to complete development and did not form infectious exoerythrocytic merozoites, thereby preventing their transition to asexual blood stage infection. Therefore, *P. falciparum mei2*$^{-}$ is a replication-competent, attenuated human malaria parasite strain with potentially increased potency, useful for vaccination to protect against *P. falciparum* malaria infection.



JCI insight

RESEARCH ARTICLE

# A replication-competent late liver stage–attenuated human malaria parasite

**Debashree Goswami,[1] William Betz,[1] Navin K. Locham,[1] Chaitra Parthiban,[2] Carolyn Brager,[1] Carola Schäfer,[1] Nelly Camargo,[1] Thao Nguyen,[1] Spencer Y. Kennedy,[1] Sean C. Murphy,[2] Ashley M. Vaughan,[1,3] and Stefan H. I. Kappe[1,3]**

[1]Center for Global Infectious Disease Research, Seattle Children's Research Institute, Seattle, Washington, USA.
[2]Department of Laboratory Medicine and [3]Department of Pediatrics, University of Washington, Seattle, Washington, USA.

**Whole-sporozoite vaccines engender sterilizing immunity against malaria in animal models and importantly, in humans. Gene editing allows for the removal of specific parasite genes, enabling generation of genetically attenuated parasite (GAP) strains for vaccination. Using rodent malaria parasites, we have previously shown that late liver stage–arresting replication-competent (LARC) GAPs confer superior protection when compared with early liver stage–arresting replication-deficient GAPs and radiation-attenuated sporozoites. However, generating a LARC GAP in the human malaria parasite *Plasmodium falciparum* (*P. falciparum*) has been challenging. Here, we report the generation and characterization of a likely unprecedented *P. falciparum* LARC GAP generated by targeted gene deletion of the *Mei2* gene: *P. falciparum mei2*$^-$. Robust exoerythrocytic schizogony with extensive cell growth and DNA replication was observed for *P. falciparum mei2*$^-$ liver stages in human liver-chimeric mice. However, *P. falciparum mei2*$^-$ liver stages failed to complete development and did not form infectious exoerythrocytic merozoites, thereby preventing their transition to asexual blood stage infection. Therefore, *P. falciparum mei2*$^-$ is a replication-competent, attenuated human malaria parasite strain with potentially increased potency, useful for vaccination to protect against *P. falciparum* malaria infection.**

## Introduction

Malaria continues to be a global threat to public health. In 2018, 228 million new cases of clinical malaria were estimated to have occurred, including 405,000 fatalities. Children under the age of 5 are the most vulnerable group, with 61% of the reported deaths (1). In malaria-endemic regions naturally acquired immunity develops after repeated episodes of malaria infection that prevents severe disease, mainly due to immunity against blood stages. In addition, there is recent evidence of immunity against the preerythrocytic stages, the sporozoite and liver stages (2–7). A highly efficacious malaria vaccine that targets the clinically silent phase of parasite infection in the liver and thereby prevents blood stage infection would not only prevent the mortality and morbidity associated with malaria disease but also block the cycle of transmission and, thus, likely be essential for ultimate malaria eradication.

The clinically most advanced malaria vaccine, RTS,S, has completed phase III clinical trials in 2014, has received a positive scientific opinion from the European Medicines Agency (Article 58) (8), and as of 2019 has begun pilot implementation in African countries (9). However, this vaccine, targeting the major surface protein, circumsporozoite protein (CSP), of the infectious sporozoite stage of *Plasmodium falciparum* (*P. falciparum*), confers only modest, relatively short-lived protection (10–15). This suggests that a monovalent subunit vaccine against a single parasite antigen might be inadequate to elicit a durable protective immune response against a complex eukaryotic pathogen with considerable strain diversity such as *P. falciparum*. Whole-organism vaccines are an alternative to subunit vaccines, and for malaria, clinical studies in the 1970s showed that *P. falciparum* radiation-attenuated sporozoites (RAS), sequentially administered to human subjects by bites of more than 1000 infected mosquitoes, engendered sterilizing immunity against a controlled human malaria infection (CHMI) consisting of 5 bites from mosquitoes carrying fully infectious *P. falciparum* sporozoites (16). Injectable formulations of metabolically active cryopreserved *P. falciparum* RAS (PfSPZ) (17), administered by direct venous inoculation, are safe and have generated robust and durable sterilizing protection against both homologous-strain

**Conflict of interest:** The authors have declared that no conflict of interest exists.



**Submitted:** December 10, 2019
**Accepted:** May 21, 2020
**Published:** July 9, 2020.

**Reference information:** *JCI Insight*. 2020;5(13):e135589. https://doi.org/10.1172/jci.insight.135589.

(18, 19) and heterologous-strain CHMI (18, 20) in malaria-naive adults. Importantly, PfSPZ is the first candidate malaria vaccine that has afforded sterilizing protection in malaria-exposed Malian adults, with a vaccine efficacy of 52% by time-to-infection analysis and 29% by proportional analysis, 6 months after the last vaccine dose (21). PfSPZs infect hepatocytes but arrest early in liver stage development and do not undergo DNA replication and significant cell growth (schizogony) because of radiation DNA damage (22, 23). PfSPZ-engendered protection involves antibodies elicited against sporozoite antigens that prevent sporozoite entry into the liver (19). More importantly however, the infection of hepatocytes by the live attenuated immunogen and presentation of liver stage antigens is thought to be essential for the generation of robust, protective $CD8^+$ T cell responses that result in elimination of infected hepatocytes (24, 25). So far, the clinical experience with PfSPZ immunization suggests that although it affords superior protection compared with current subunit vaccines, it does not confer complete protection in areas of endemic malaria transmission (21) and therefore requires improvement. This might be achieved by creating a whole-parasite immunogen that actively replicates in the liver, thereby generating considerably increased antigen breadth and biomass, which when presented to the host's immune system, engenders superior immune protection (26, 27). Indeed, proof-of-concept CHMI clinical trials with chemoprophylaxis with sporozoites (CPS) showed that allowing full liver stage development of the immunogen generates durable sterilizing protection at a dose one-twentieth of that used with the PfSPZ vaccine (28, 29).

Over the last 2 decades, significant advances in genetic engineering have made the generation of transgenic *Plasmodium* parasites possible. CRISPR/Cas gene editing has increased the efficiency and reliability of parasite genetic manipulation in more recent years (26). Introducing targeted gene deletions into the complex parasite genome of more than 5000 genes enables the generation of genetically attenuated parasites (GAPs) that specifically arrest their growth during hepatocyte infection (26). First-generation GAPs consisted of early liver stage–arresting replication-deficient (EARD) parasites that harbored deletions of genes involved in regulating the early phases of hepatocyte infection (30, 31). Numerous EARD GAPs were first generated in rodent malaria parasites, but few of the discovered gene deletions were successfully used to create viable, liver stage–attenuated *P. falciparum* EARD GAPs (32, 33). This is likely due to the highly divergent nature of the human malaria parasite and rodent malaria parasite genomes, separated by millions of years of evolution, rendering the discovery of genes that share identical functions a challenge (34, 35). In consequence only 3 *P. falciparum* EARD GAP strains have been generated to date (32, 33, 36), and 1, *P. falciparum* GAP3KO (*P. falciparum p52*$^-$*/p36*$^-$*/sap1*$^-$), has so far shown to be completely attenuated in a human trial (28).

The aforementioned superior efficacy against CHMI in humans immunized with replication-competent *P. falciparum* CPS compared with replication-deficient *P. falciparum* RAS encourages the quest for the development of late liver stage–arresting replication-competent (LARC) GAP strains for vaccination. However, the identification of gene deletions in *P. falciparum* that arrest parasite development late during liver stage schizogony has proved extremely challenging (37). In this study, we focused our efforts on the late liver stage–expressed gene *P. falciparum Mei2*, for which orthologs in other organisms have functions in DNA segregation and cell division (38). We report here that the deletion of *P. falciparum Mei2* generates a *P. falciparum* LARC GAP.

## Results

*P. falciparum Mei2 is expressed during liver stage development*. We have previously reported that *Plasmodium yoelii* (*P. yoelii*) PlasMei2 is expressed only during late phases of liver stage development (38). We thus screened previously published *P. falciparum* data sets for expression of *P. falciparum Mei2* transcript and protein in asexual blood stages, gametocytes, oocysts, and salivary gland sporozoites and found one report for expression in gametocytes (39). We next analyzed expression of *P. falciparum Mei2* transcripts in *P. falciparum* liver stages using the highly sensitive RNAscope in situ hybridization technology (40) with a *P. falciparum Mei2*–specific probe, a methodology heretofore not used, to our knowledge, to detect transcripts in *P. falciparum* parasite tissue schizonts. Fah$^{-/-}$RAG2$^{-/-}$IL2rg$^{-/-}$ (FRG) mice repopulated with primary human hepatocytes (FRG huHep) (41) were infected with 1 million WT *P. falciparum* NF54 sporozoites, and infected livers were removed at different time points of liver stage development and subjected to tissue sectioning. RNAscope of *P. falciparum Mei2* transcripts detected expression in liver stages on days 4, 5, 6, and 7 postinfection as punctate dots distributed throughout the cytoplasm of liver stage schizonts (Figure 1). Transcripts for *P. falciparum HSP70*, used as a positive control, could also be detected. To further

evaluate the spatiotemporal localization of the PlasMei2 protein, we generated a transgenic *P. falciparum Mei2*–mCherry parasite line expressing PlasMei2 with a C-terminal fusion mCherry tag using CRISPR/Cas9 gene editing tools (Supplemental Figure 3; supplemental material available online with this article; https://doi.org/10.1172/jci.insight.135589DS1). Two independent *P. falciparum Mei2*–mCherry clones were used for phenotypic analysis. No expression of mCherry was seen in the asexual stages, in gametocytes, and during mosquito stage development (data not shown). To analyze expression of PlasMei2 in the liver, 1 million sporozoites from one of the *P. falciparum Mei2*–mCherry clones were used to infect FRG huHep mice, and livers were harvested between days 4 and 7 and analyzed by immunofluorescence assay (IFA). An antibody against mCherry was used to detect expression of PlasMei2, and an antibody against the endoplasmic reticulum (ER) marker, BiP, was used to identify liver stage parasites. PlasMei2 protein expression was not detected in day 4 liver stages, but expression was observed on days 5, 6, and 7 postinfection with the highest expression seen on days 6 and 7 (Figure 2). PlasMei2 expression was localized to the liver stage interior and displayed a granular expression pattern on day 7. These results indicate that the PlasMei2 protein is expressed between days 5 and 7 during *P. falciparum* liver stage schizogony.

*Generation of P. falciparum Mei2–deficient parasites*. To investigate the role of the *P. falciparum* PlasMei2 protein throughout the parasite life cycle, we generated *P. falciparum mei2*$^-$ parasites in the *P. falciparum* NF54 WT strain via CRISPR/Cas9-mediated gene editing using a plasmid backbone, pFC, generated in a manner similar to the pYC plasmid previously shown to successfully create *P. yoelii* transgenic parasites (42) (Figure 3A and Supplemental Figure 1A). The construct comprises the *P. falciparum* U6 promoter driving expression of the sgRNA cassette; the *P. falciparum* EF1α promoter driving the positive selection marker, *hDHFR*, as well as *Streptococcus pyogenes* (*S. pyogenes*) *Cas9* as a bicistronic transcript separated by a 2A viral skip peptide; and a multiple cloning site for cloning the repair templates for recombination. The pFC-PlasMei2 plasmid was generated by cloning homology repair templates for *Mei2* and an *Mei2*-specific guide into the pFC plasmid (Supplemental Table 1). This plasmid was transfected into NF54 parasites. Transfected parasites were screened for the correct recombination pattern using PCR genotyping, and recombinant parasite populations were used for cloning by limiting dilution (Figure 3A). *P. falciparum mei2*$^-$ clones F2 and F5 were used for further phenotypic characterization. Deletion of *P. falciparum Mei2* was also further confirmed by Southern blot analysis (Figure 3B). Loss of *P. falciparum Mei2* expression in *P. falciparum mei2*$^-$ liver stages was confirmed by performing RNAscope, which also validated the specificity of the *P. falciparum Mei2*–specific probe (Supplemental Figure 2).

*P. falciparum mei2*$^-$ *parasites undergo normal asexual blood stage development, gametocytogenesis, and mosquito stage development*. Asexual blood stage parasitemias of *P. falciparum mei2*$^-$ clones F2 and F5 were measured over 3 replication cycles and compared with the parental *P. falciparum* NF54 parasites. No significant difference in growth was observed between the *P. falciparum mei2*$^-$ clones and *P. falciparum* NF54, indicating that *P. falciparum* PlasMei2 is dispensable for asexual blood stage growth and replication (Figure 3C). *P. falciparum mei2*$^-$ parasites also did not display any defects in the commitment to gametocytogenesis, the maturation of male and female gametocytes, and the formation of motile male gametes (data not shown). Next, *P. falciparum mei2*$^-$ and *P. falciparum* NF54 gametocyte cultures were transmitted to *Anopheles stephensi* mosquitoes by standard membrane feeding. The prevalence of *P. falciparum mei2*$^-$ mosquito midgut infection was indistinguishable from parental *P. falciparum* NF54 infections (Figure 3D). Importantly, the numbers of oocysts and salivary gland sporozoites per infected mosquito were comparable between *P. falciparum* NF54 and *P. falciparum mei2*$^-$ clone F2 (Figure 3, E and F). We observed lower oocyst numbers and lower salivary gland sporozoite numbers per mosquito for clone F5 when the mean of 3 independent experiments was compared with *P. falciparum* NF54. However, this difference was not statistically significant. One experiment yielded 18,000 F5 sporozoites per mosquito, indicating that this clone can produce robust sporozoite numbers. Furthermore, oocyst prevalence and oocyst and sporozoite counts per mosquito for a third *P. falciparum mei2*$^-$ clone were also comparable to *P. falciparum* NF54 (data not shown). The range of sporozoite loads in the mosquitoes between experiments is thus most likely caused by variability in mosquito infection rates, which in turn depend on the quality of the gametocyte culture used for feedings. We conclude that *P. falciparum* PlasMei2 does not exert an important function in the parasite blood stages and mosquito stages and has no significant role in sporogony or infection of the mosquito salivary glands.

*P. falciparum mei2*$^-$ *liver stages undergo nearly complete exoerythrocytic schizogony but do not form exoerythrocytic merozoites*. To explore the role of *P. falciparum Mei2* in liver stage development, 1 million *P. falciparum mei2*$^-$

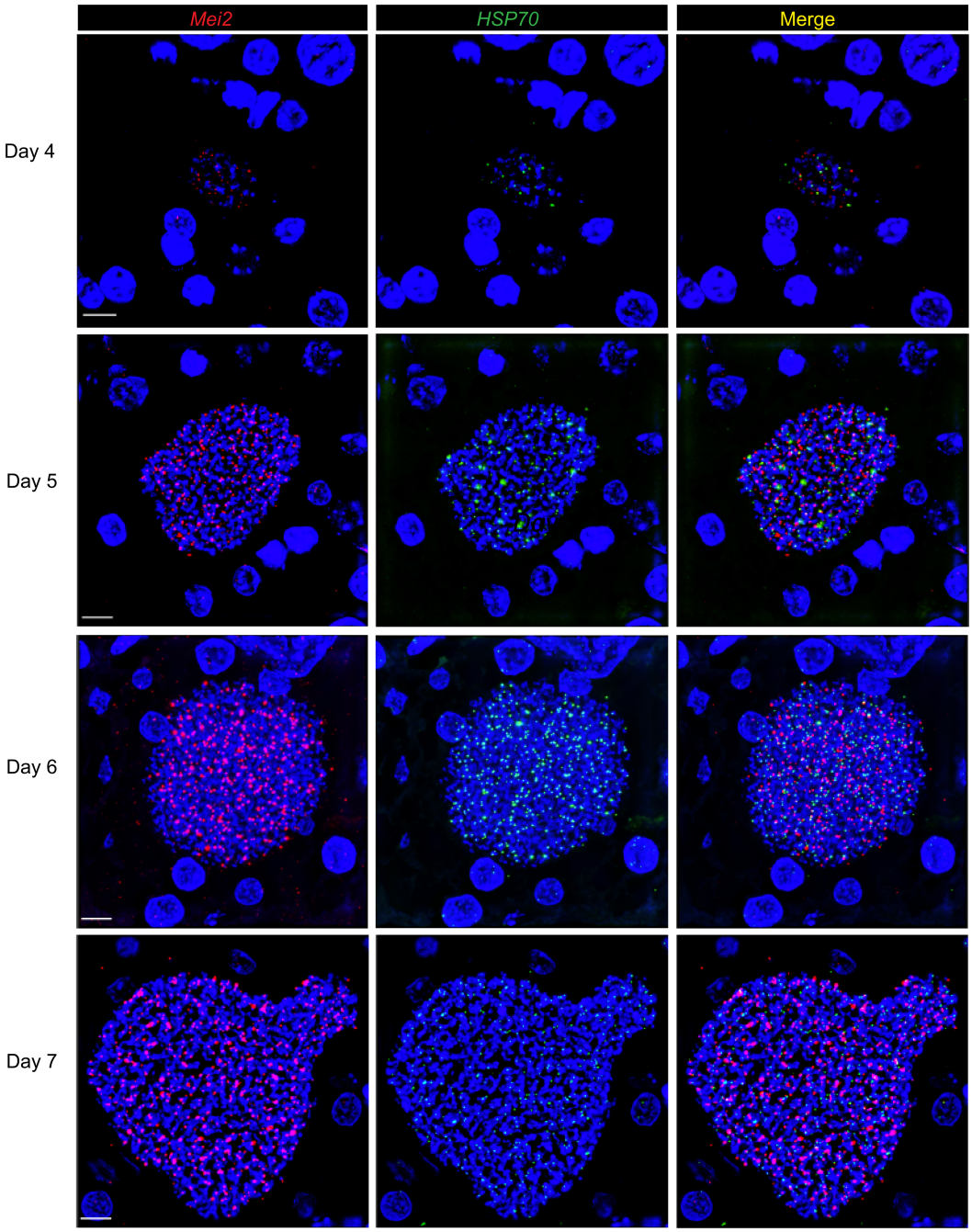


**Figure 1. *P. falciparum Mei2* transcripts are detected in *P. falciparum* liver stages.** Liver tissue sections from FRG NOD huHep mice infected with *P. falciparum* NF54 sporozoites were prepared on days 4, 5, 6, and 7 of liver stage development and analyzed by RNAscope. Probes targeting *P. falciparum Mei2* (shown in red) and *P. falciparum HSP70* (shown in green) as a control are shown. DNA is visualized by staining with DAPI (shown in blue). The 2 transcripts were detected at all 4 time points of liver stage schizogony. Scale bar: 7 μm.

or *P. falciparum* NF54 sporozoites were injected intravenously into FRG huHep mice (43). Infected livers were harvested at different time points postinfection to qualitatively and quantitatively assess liver stage development by IFA. Early-to-mid liver stage development 3–5 days postinfection was studied using antibodies against CSP, which marks the parasite plasma membrane (PPM), and against the ER marker, BiP (Supplemental Figure 4). *P. falciparum mei2*$^{-}$ sporozoites infected hepatocytes and formed intrahepatocytic trophozoites. This early stage of hepatocyte infection as well as early- to mid-stage schizogony was indistinguishable from *P. falciparum* NF54 parasites up to day 5 after sporozoite infection. However, from day 6 onward, clear developmental differences between WT and *P. falciparum mei2*$^{-}$ liver stages emerged (Figure 4).

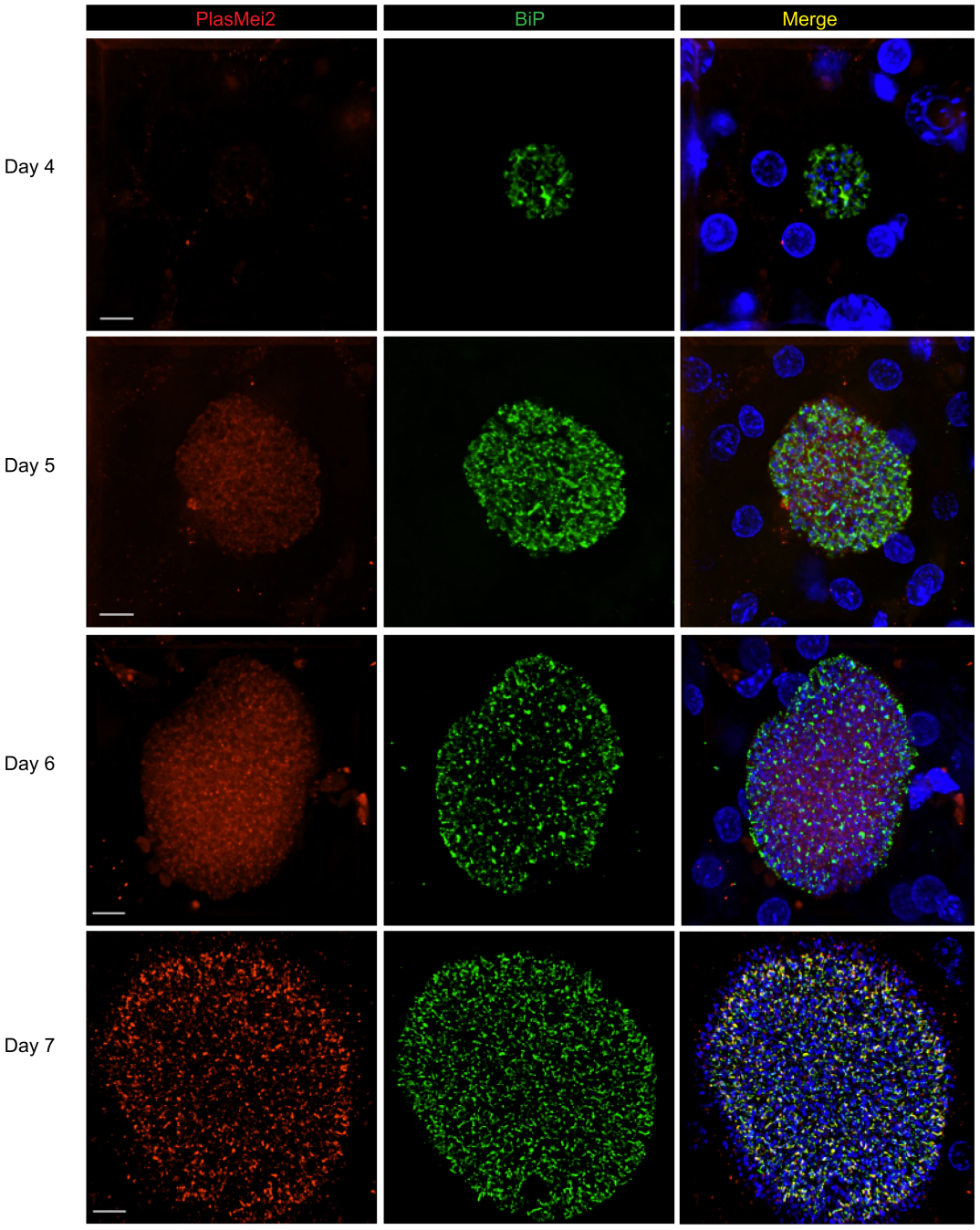


**Figure 2. PlasMei2 protein is expressed in mid-to-late liver stage schizonts.** Liver tissue sections from FRG NOD huHep mice infected with *P. falciparum Mei2*–mCherry sporozoites were prepared on days 4, 5, 6, and 7 of liver stage development and analyzed by IFA. Liver stage parasites were visualized using antibodies against the parasite ER marker, BiP (green). PlasMei2 was detected using an anti-mCherry antibody (red). DNA was visualized using DAPI (blue). PlasMei2 protein was not expressed on day 4 of liver stage development. Expression was observed in mid-to-late liver stage schizonts on days 5, 6, and 7. Scale bar: 7 μm.

While *P. falciparum* NF54 liver stage schizonts significantly increased in size from day 6 to day 7, the *P. falciparum mei2*$^-$ liver stage schizonts suffered an apparent growth arrest from day 6 onward (Figure 4A). Next, total parasite biomass in the liver was determined on days 6 and 7 postinfection by using qRT-PCR of *P. falciparum* 18S rRNA (Figure 4B). Interestingly, biomass of *P. falciparum mei2*$^-$ liver infection on days 6 and 7 was comparable to *P. falciparum* NF54. These results indicate that *P. falciparum mei2*$^-$ exhibits similar infectivity for human hepatocytes when compared with *P. falciparum* NF54 but suffers an apparent growth defect very late in liver stage development.

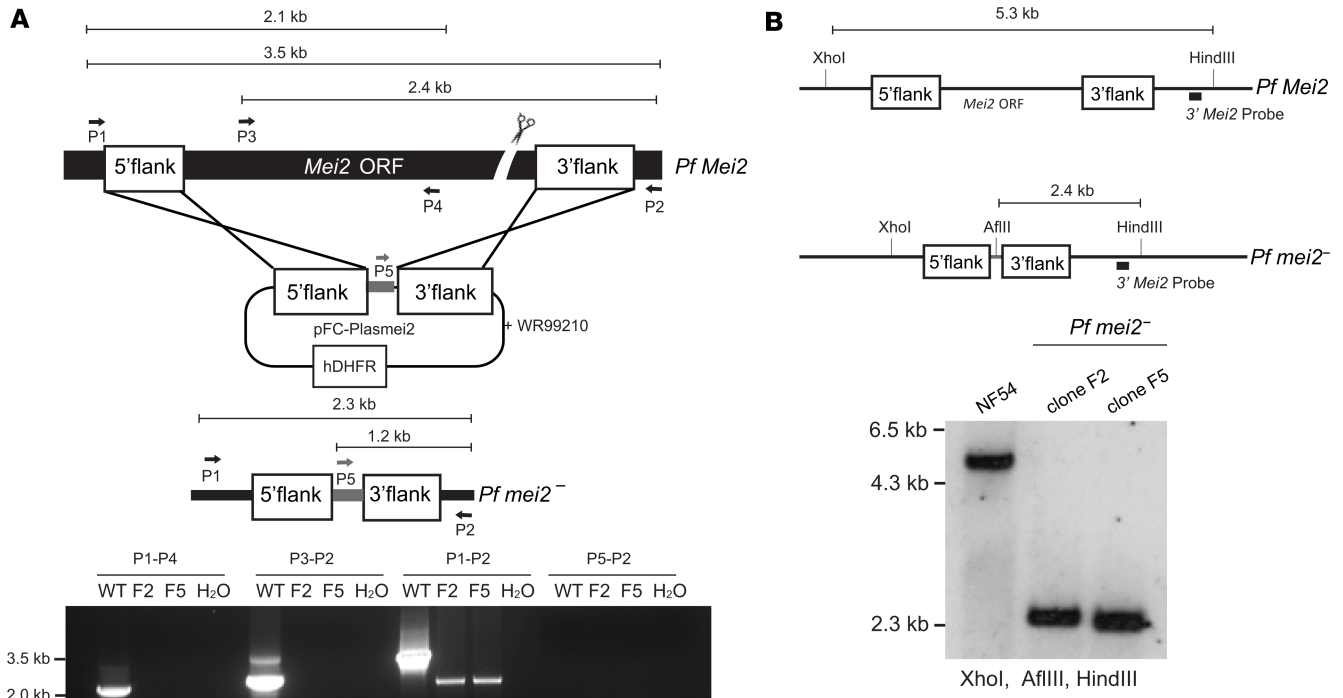


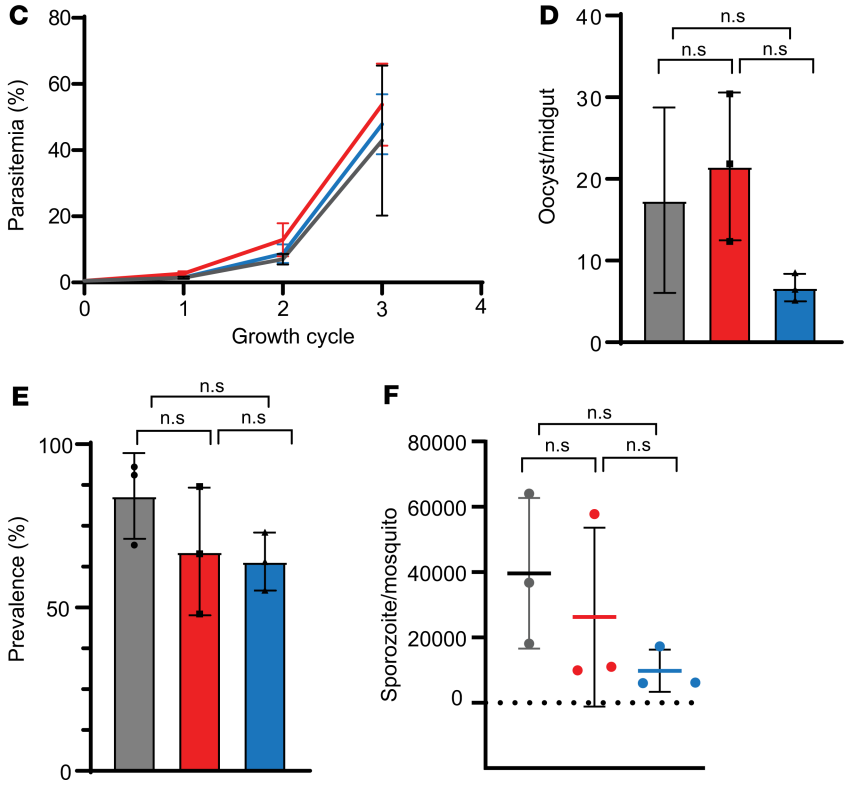


**Figure 3. *P.falciparum mei2*⁻ parasites have no defects in blood stage and mosquito stage development.** (**A**) The schematic depicts the generation of the *P. falciparum mei2*⁻ parasite using CRISPR/Cas9-mediated gene editing. Primers used to verify the gene deletion are indicated, and the sizes of the PCR products are shown in kilobases. Agarose gel electrophoresis shows the PCR products corresponding to the gene deletion *P. falciparum mei2*⁻ clones F2 and F5. *hDHFR*, human dihydrofolate reductase. (**B**) The schematic (upper right) and the corresponding Southern blot for the *P. falciparum* NF54 and *P. falciparum mei2*⁻ locus. The genomic DNA for *P. falciparum* NF54 and *P. falciparum mei2*⁻ clones F2 and F5 was digested with XhoI, HindIII, and AflIII and probed with the 3′ *Mei2* probe. (**C**) Asexual blood stage parasitemia is compared between *P. falciparum* NF54 (gray line) and *P. falciparum mei2*⁻ clones F2 (red line) and F5 (blue line) over 3 replication cycles. Data represent mean ± SD. $n = 3$ biological replicates. Statistical analysis was carried out using 2-way ANOVA. ns, not significant. $P > 0.05$ is taken as ns. Graphs comparing (**D**) the counts for oocyst/midgut, (**E**) oocyst prevalence, and (**F**) counts for sporozoites/mosquito for *P. falciparum* NF54 (gray) and *P. falciparum mei2*⁻ clones F2 (red) and F5 (blue). Data represent mean ± SD. $n = 3$ biological replicates. Statistical analysis was carried out using 1-way ANOVA. $P > 0.05$ is taken as ns.

To phenotype *P. falciparum mei2*$^-$ liver stages at the cellular level, we performed IFAs on late liver stage schizonts on days 6 and 7 postinfection. Maturation of liver stage schizonts is characterized by multiple invaginations of the PPM, resulting in a significant increase in membrane surface area, a process called cytomere formation. This process gives the schizont a walnut-like appearance and precedes the compartmentalization of cytoplasm and organelles necessary for formation of exoerythrocytic merozoites (44). Cytomere formation was visible in *P. falciparum* NF54 parasites starting on day 6 postinfection as CSP-marked PPM invaginations that surrounded a ring of nuclear DNA centers (Figure 5A). Strikingly, *P. falciparum mei2*$^-$ liver stages on day 6 exhibited extremely aberrant cytomere formation. CSP-localized PPM invaginations were virtually undetectable, and the PPM was disorganized (Figure 5A). On day 7 of liver stage development, *P. falciparum* NF54 schizonts continued to mature with distinct cytomeres visible throughout the cell. In contrast, *P. falciparum mei2*$^-$ differentiation had ceased, and membrane invaginations remained absent (Figure 6A). We confirmed this phenotype by staining for the merozoite surface protein-1 (MSP-1), which is expressed on the PPM of late schizonts and mature merozoites (Supplemental Figure 5). In contrast to *P. falciparum* NF54 liver stages, *P. falciparum mei2*$^-$ liver stages exhibited scattered and diffused MSP-1 staining throughout the schizont, further substantiating an extreme developmental defect late in schizogony.

Liver stage schizogony also requires extensive amplification and branching of the ER, mitochondria, and apicoplast, followed by their fission and segregation into daughter merozoites (44, 45). The developmental morphology of these organelles was studied using antibodies against BiP (ER marker), mHSP70 (mitochondrial marker), and ACP (apicoplast marker). On day 6 of *P. falciparum* NF54 liver stage development, the ER was extensively branched and appeared to partition into cytomere folds. In contrast *P. falciparum mei2*$^-$ liver stages showed a completely disorganized and scattered ER (Figure 5A). The apicoplast and mitochondria displayed extensive branching in *P. falciparum* NF54 parasites on day 6, and a similar pattern was also observed in *P. falciparum mei2*$^-$ without any apparent impairments in morphology of these 2 organelle complexes (Figure 5B). On day 7 of liver stage development, the *P. falciparum mei2*$^-$ liver stage ER continued to develop in striking difference to NF54, the latter of which appeared highly organized and partitioned (Figure 6A). The mitochondria and apicoplasts in *P. falciparum mei2*$^-$ remained branched but appeared to involute when compared with day 6. In contrast the mitochondria and apicoplasts in *P. falciparum* NF54 had massively multiplied and appeared segregated for partitioning into daughter merozoites (Figure 6B). By day 8, very few *P. falciparum mei2*$^-$ parasites were detected, and these parasites had not undergone further differentiation (Supplemental Figure 7). The liver stage phenotype observed in *P. falciparum mei2*$^-$ parasites was similar for both the clones analyzed (Supplemental Figure 6).

Exoerythrocytic schizogony is characterized by multiple rounds of DNA replication and segregation in the absence of immediate cytokinesis within a coenocyte-like cell. This creates tens of thousands of individualized genomes (DNA centers), which are ultimately each allocated into daughter merozoites (46) (Figure 7). In our analysis of *P. falciparum mei2*$^-$ liver stage development, we observed a strong defect in the extent of DNA replication on day 7 (Figure 6). To investigate this further, DAPI-stained DNA centers were compared between *P. falciparum* NF54 and *P. falciparum mei2*$^-$ at day 7 of liver stage development (Figure 7A). *P. falciparum mei2*$^-$ showed fewer DNA centers, although this difference was not statistically significant. *P. falciparum mei2*$^-$ schizonts contained fewer than 5000 centers, while *P. falciparum* NF54 schizonts contained up to 15,000 centers (Figure 7B). In addition, we found that the volume occupied by each DNA center was significantly less in *P. falciparum mei2*$^-$ compared with *P. falciparum* NF54 (Figure 7C). These data provide evidence that DNA replication and segregation are impaired because of the lack of *P. falciparum Mei2*.

Together, these results demonstrate that *P. falciparum* PlasMei2 is required for completion of liver stage development, by playing a role in schizont maturation, and the ultimate formation of mature exoerythrocytic merozoites.

*P. falciparum mei2*$^-$ *liver stage schizonts fail to produce infectious exoerythrocytic merozoites*. We further explored the severity of the *P. falciparum mei2*$^-$ liver stage developmental defect by asking whether these parasites at all mature into exoerythrocytic merozoites that can infect human RBCs. This constitutes the essential step for transition from the asymptomatic liver stage of infection to the symptomatic blood stage infection. Transition to blood stage infection is also the most sensitive measure for detecting possible parasite breakthrough because very few infectious exoerythrocytic merozoites are required to successfully initiate the blood stage infection of the life cycle. As previously reported, in FRG huHep mice,

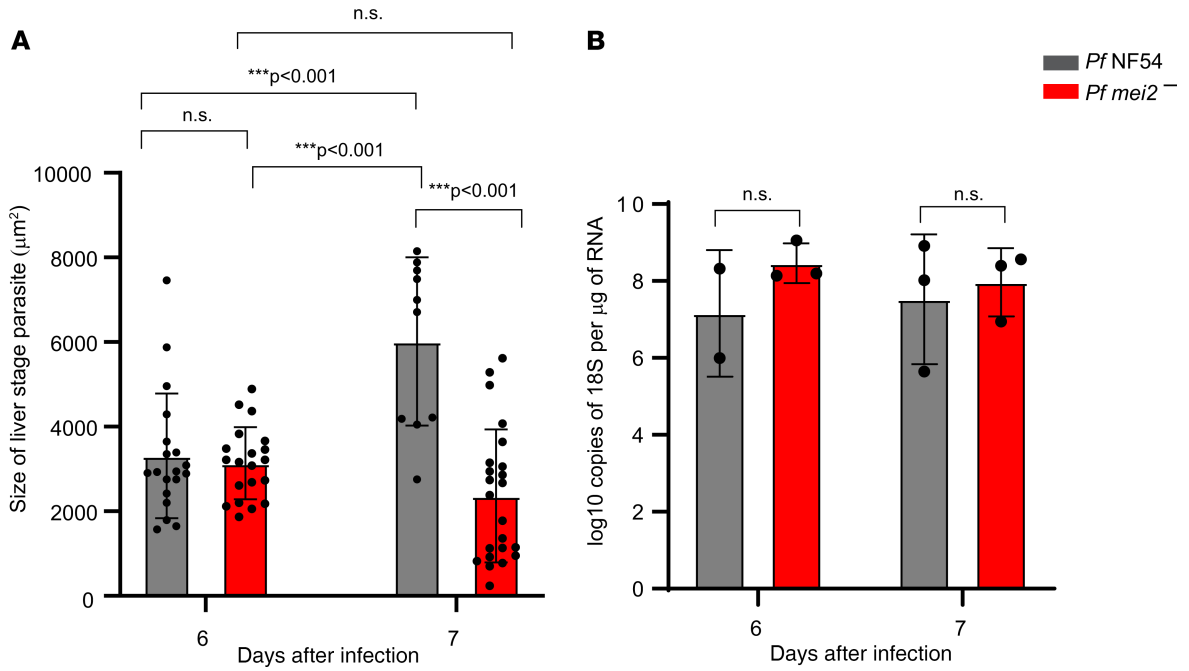


**Figure 4. *P. falciparum mei2*⁻ liver stages display late defects in exoerythrocytic schizogony.** *P. falciparum* NF54 and *P. falciparum mei2*⁻ sporozoites were injected intravenously into FRG NOD huHep mice, and infected liver tissue sections were used for measuring parasite size by IFA and parasite rRNA load by 18S rRNA quantitative real-time PCR (qRT-PCR). (**A**) Comparison of the size of late liver stage parasites (based on area at the parasite's largest circumference) between *P. falciparum* NF54 (gray) and *P. falciparum mei2*⁻ (red) on days 6 and 7 postinfection. *P. falciparum* NF54 liver stages are significantly larger than *P. falciparum mei2*⁻ on day 7. Data represent mean ± SD. *n* = at least 12 schizonts per time point. Statistical analysis was carried out using 2-way ANOVA using Tukey's multiple comparison test. *P* values are indicated in the graph. $P > 0.05$ is taken as ns. (**B**) Analysis of parasite liver load by 18S rRNA qRT-PCR was carried out on extracted RNA from *P. falciparum* NF54–infected (gray) and *P. falciparum mei2*⁻–infected (red) livers on day 6 and 7 postinfection, depicted as $\log_{10}$ copies of *P. falciparum* 18S rRNA/µg of extracted liver RNA. Data represent mean ± SD. *n* = 3 mice per time point. Statistical analysis was carried out using 2-way ANOVA using Holm-Šídák multiple comparison test. *P* values are indicated in the graph. $P > 0.05$ is taken as ns.

*P. falciparum* NF54 liver stages can transition to a blood stage infection when human RBCs are injected toward the completion of liver stage development (47–49). These infected RBCs can be transferred to in vitro culture, where parasites undergo asexual schizogony and can be detected by Giemsa-stained thin blood smears within 1 to 5 days of culture (48). Alternatively, parasite nucleic acid can be detected by a highly sensitive parasite 18S qRT-PCR assay (50, 51). This has been used as a diagnostic tool to detect the presence of blood stage parasites in human blood samples following CHMI (52). The assay is capable of detecting as few as 1 ring stage parasite equivalent in 50 µL of blood sample, which comprises 3.86 $\log_{10}$ copies of 18S rRNA/mL of blood (50).

We conducted 2 independent experiments to assess the severity of liver stage attenuation of *P. falciparum mei2*⁻. In the first experiment, we injected 1 million *P. falciparum* NF54 sporozoites and 1 million *P. falciparum mei2*⁻ clone F2 sporozoites into 2 and 4 FRG huHep mice each, respectively (Figure 8A). To enable liver stage–to–blood stage transition, we intravenously (i.v.) injected human RBCs on days 6 and 7 as previously described (47). Blood samples (50 µL) were then removed for 18S qRT-PCR every day from days 7 through 10. On day 7, 500 µL of blood was drawn and transferred to in vitro culture to allow asexual parasite replication in culture. On day 10, all mice were euthanized and exsanguinated by cardiac puncture, and the blood was transferred to in vitro culture again. In the 2 FRG huHep mice injected with NF54 sporozoites, we detected 18S rRNA by qRT-PCR from days 7 through 10 (Table 1 and Supplemental Figure 8A). The qRT-PCR on day 7 showed 8.39 and 8.61 $\log_{10}$ 18S copies of rRNA/mL of blood for the 2 mice (33,000 and 55,000 parasite equivalents/mL). Parasites were detected by Giemsa-stained thin blood smears within 1 to 3 days after transfer to in vitro culture on days 7 and 10. In contrast, 3 of 4 mice infected with *P. falciparum mei2*⁻ sporozoites were blood stage negative by qRT-PCR, and 1 mouse showed extremely low blood stage positivity by qRT-PCR of 4.95 $\log_{10}$ copies of 18S rRNA/mL of blood (32 parasite equivalents/mL) on day 7 (Table 1 and Supplemental Figure 8A). All 4 mice were blood stage negative by qRT-PCR from days 8 to 10. Furthermore, we did not detect any parasites by Giemsa-stained thick smears

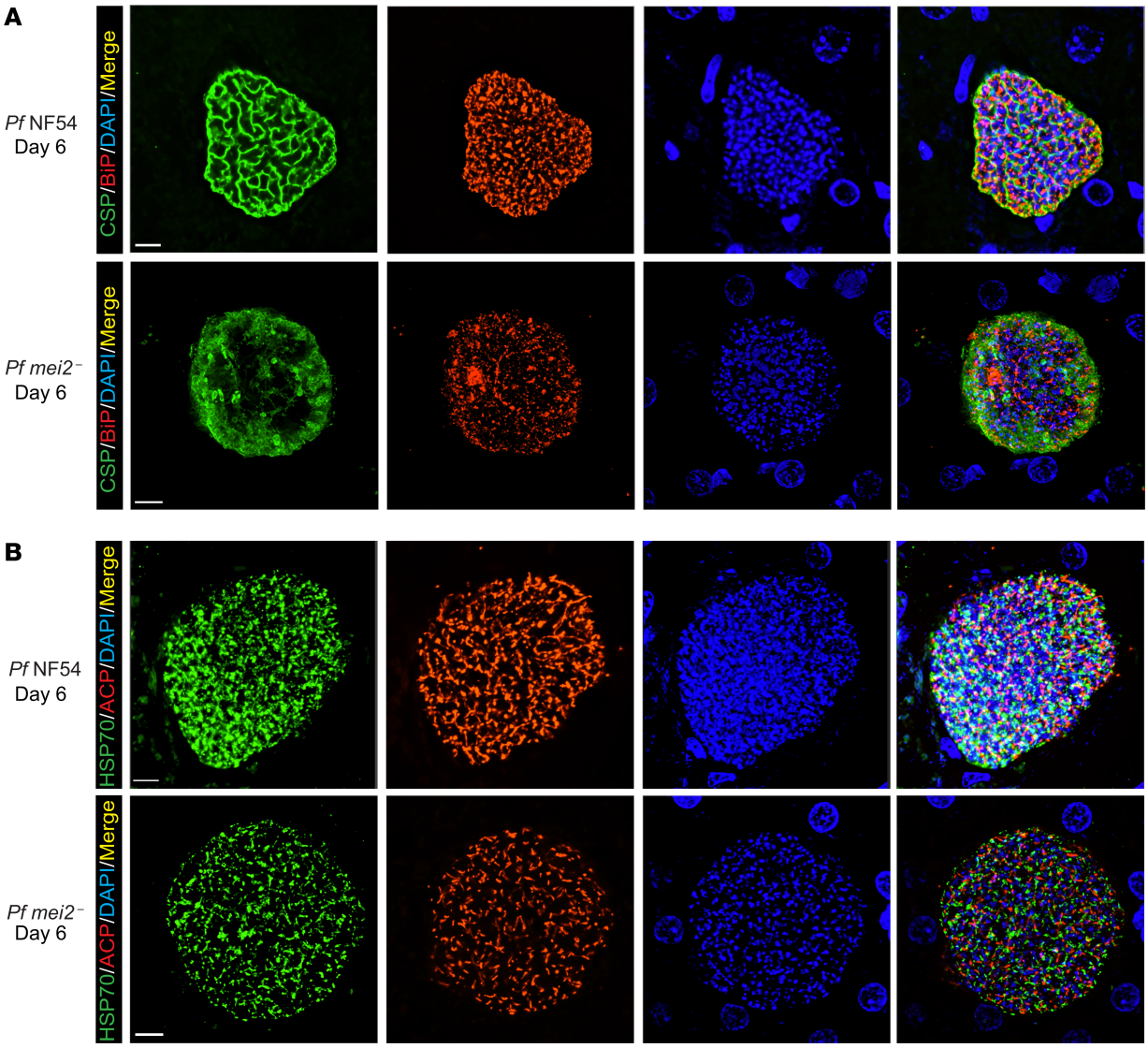


**Figure 5. *P. falciparum mei2*⁻ late liver stages display defects in cytomere formation.** Liver tissue sections from FRG NOD huHep mice infected with *P. falciparum* NF54 or *P. falciparum mei2*⁻ sporozoites were prepared on day 6 of liver stage development and used for IFA. (**A**) IFA using an antibody against CSP (green), which delineates the PPM of *P. falciparum* NF54 day 6 liver stages (upper panel), shows membrane invaginations typical of cytomere formation. CSP-positive PPM invaginations are lacking in *P. falciparum mei2*⁻ liver stages (lower panel). The ER was delineated using an antibody against BiP (red) and was aberrant in *P. falciparum mei2*⁻. DNA was localized with DAPI (blue). (**B**) IFAs were carried out to compare development of parasite organelles, including the mitochondria (mHSP70, green) and apicoplast (ACP, red), between *P. falciparum* NF54 (upper panel) and *P. falciparum mei2*⁻ (lower panel) on day 6. The mitochondria and apicoplast development appear normal in *P. falciparum mei2*⁻ day 6 liver stages. Scale bar: 7 μm.

(more sensitive than thin blood smears) in blood transferred to in vitro culture on days 7 and 10 from all 4 mice. After 10 days of in vitro culture, blood samples analyzed from the cultures were all negative for parasites by qRT-PCR and Giemsa-stained thick smear.

It has been previously shown that the presence of a mutation in the SIRPα gene in the NOD background of mice leads to superior engraftment of human cells, by preventing mouse macrophages from clearing the graft (48). Due to the SIRPα polymorphism, FRG NOD mice are more amenable to human RBC repopulation compared with FRG mice. Thus, in a second experiment, we further investigated *P. falciparum mei2*⁻ liver stage–to–blood stage transition using FRG NOD huHep mice infected with *P. falciparum mei2*⁻ clones F2 and F5. One million sporozoites from *P. falciparum* NF54 and *P. falciparum mei2*⁻ clones F2 and F5 were injected i.v. into 2, 2, and 4 FRG NOD huHep mice, respectively (Figure 8B). On day 7 post-infection, 50 μL of blood was sampled for qRT-PCR from all 8 mice. Five mice were euthanized on day 7 (1 mouse injected with NF54, 1 injected with clone F2, and 3 injected with clone F5), and blood was drawn

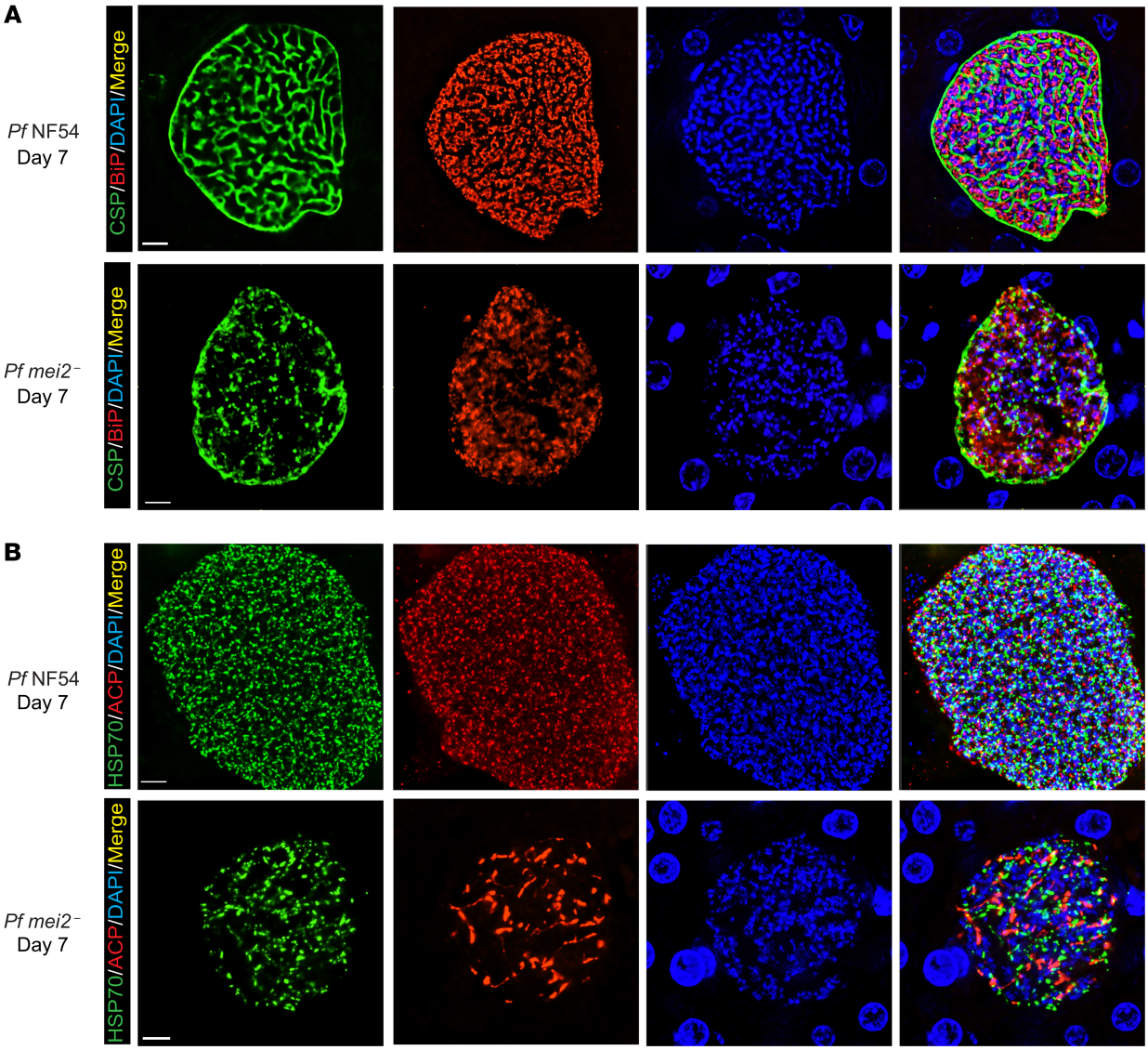


**Figure 6. *P. falciparum mei2*⁻ day 7 liver stages display severe differentiation defects and cannot form exoerythrocytic merozoites.** Liver tissue sections from FRG NOD huHep mice infected with *P. falciparum* NF54 or *P. falciparum mei2*⁻ sporozoites were prepared on day 7 of liver stage development and used for IFA. (**A**) IFAs for CSP (green), BiP (red), and DNA (blue) in *P. falciparum* NF54 day 7 liver stages show further maturation and formation of distinct PPM invaginations preceding the development of exoerythrocytic merozoites (upper panel) while CSP localization for *P. falciparum mei2*⁻ is aberrant (lower panel). In *P. falciparum* NF54 there is pronounced segregation of the ER in preparation for exoerythrocytic merozoite formation, but this does not occur in *P. falciparum mei2*⁻. (**B**) IFAs comparing development of the organelles mitochondria (mHSP70, green) and apicoplast (ACP, red) between NF54 (upper panel) and *P. falciparum mei2*⁻ (lower panel) on day 7. The mitochondria and apicoplast have undergone segregation inside exoerythrocytic merozoites in *P. falciparum* NF54, while in *P. falciparum mei2*⁻ they remain branched and do not segregate. Scale bar: 7 μm.

by cardiac puncture and transferred to in vitro culture. The remaining 1 mouse for *P. falciparum* NF54 and clones F2 and F5 was euthanized and exsanguinated on day 8, and blood was transferred to in vitro culture.

Both FRG NOD mice infected with *P. falciparum* NF54 were qRT-PCR positive on day 7 with 7.7 and 9.6 $\log_{10}$ copies of 18S rRNA copies/mL of whole mouse blood (6830 and 540,000 parasite equivalents/mL) (Table 2 and Supplemental Figure 8B). For the 1 mouse exsanguinated on day 7, in vitro culture of the transferred blood was positive by thin smear within 4 days of culture. For the second mouse exsanguinated on day 8, there were 10.21 $\log_{10}$ copies of 18S rRNA copies/mL of mouse blood ($2.2 \times 10^6$ parasite equivalents/mL) by qRT-PCR. Parasites could be detected on thin smear within 1 day after transfer of blood to in vitro culture.

One of 2 FRG NOD huHep mice infected with *P. falciparum mei2*⁻ clone F2 was qRT-PCR positive with 7.05 $\log_{10}$ copies of 18S rRNA copies/mL of whole mouse blood (1573 parasite equivalents/mL) on day 7 (Table 2 and Supplemental Figure 8B). In vitro culture of blood drawn from this mouse and cultured for 8

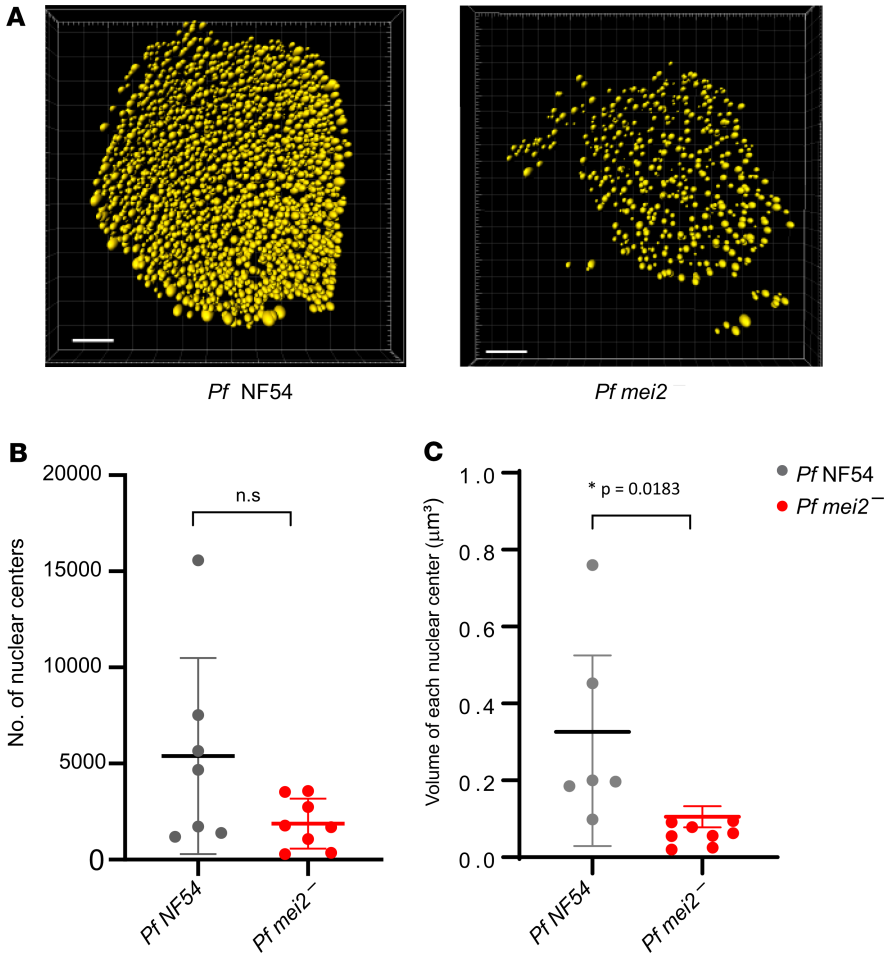


**Figure 7. *P. falciparum mei2*⁻ liver stages display defects in DNA replication and segregation.** (**A**) An analysis of nuclear DNA centers based on DAPI staining between NF54 and *P. falciparum mei2*⁻ liver stages on day 7. Scale bar: 7 μm. (**B**) The graph shows the total number of nuclear centers per late liver stage schizont. Fewer nuclear centers are observed in *P. falciparum mei2*⁻ (red) in comparison with *P. falciparum* NF54 (gray), indicating incomplete DNA segregation. Data represent mean ± SD. $n = 7$ liver stage schizonts. Statistical analysis was carried out using an unpaired $t$ test. $P > 0.05$ is taken as ns. (**C**) The graph shows the volume of each nuclear center. The average volume per nuclear center was calculated for each schizont (day 7). *P. falciparum mei2*⁻ (red) nuclear centers are smaller in comparison with *P. falciparum* NF54 (black), indicating less DNA content in *P. falciparum mei2*⁻. These results indicate a defect in DNA replication and segregation. Data represent mean ± SD. $n = 7$ liver stage schizonts. Statistical analysis was carried out using an unpaired 2-tailed $t$ test. $P$ value is mentioned in the graph. $P > 0.05$ is taken as ns.

weeks, however, did not lead to any detectable parasitemia as determined by thick smear. In addition, samples from in vitro culture that were analyzed by qRT-PCR for parasite 18S rRNA every week for 8 weeks were also negative. No 18S rRNA was detected by qRT-PCR from the second mouse on day 8, and no parasites were detected by thick smears in blood drawn from this mouse and maintained in culture for 8 weeks. Additionally, no 18S rRNA was detected in samples drawn from in vitro culture every week for 8 weeks. All 4 mice infected with clone F5 were negative for parasite 18S rRNA by qRT-PCR on day 7. For the 3 mice exsanguinated on day 7, in vitro culture of blood drawn from these mice and cultured for 8 weeks did not show any detectable parasitemia as determined by thick smears. For the 1 mouse exsanguinated on day 8, no 18S rRNA was detected in blood, and no parasites could be recovered after 8 weeks of in vitro culture. Samples from in vitro culture analyzed by qRT-PCR for the presence of parasite nucleic acids every week for 8 weeks for all 4 replicates were also negative.

Thus, only 2 of 10 FRG huHep/FRG NOD huHep mice infected with 1 million *P. falciparum mei2*⁻ sporozoites showed presence of any 18S rRNA (32 and 1573 parasite equivalents/mL) in the blood once and only on day 7 (Table 3) at a time when *P. falciparum mei2*⁻ liver stages had suffered a growth defect late in liver stage schizogony. The same diagnostic qRT-PCR assay has been used as the endpoint in CHMI

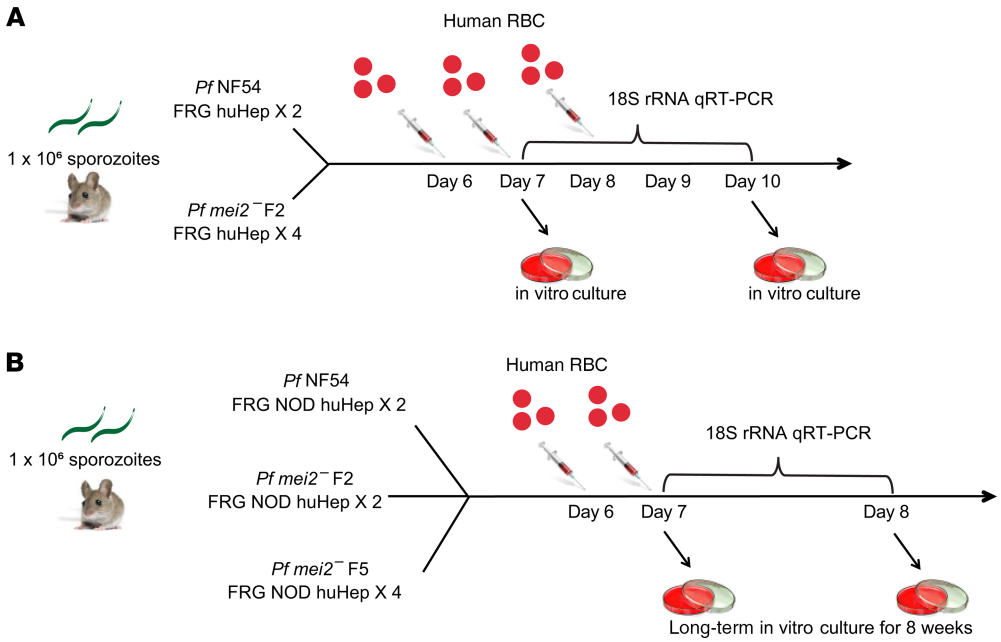


**Figure 8. Experimental design for testing *P. falciparum mei2*⁻ liver stage breakthrough to blood stage patency.** (**A**) Schematic represents the experimental setup for results shown in Table 1 and in Supplemental Figure 8A. One million sporozoites from *P. falciparum* NF54 or *P. falciparum mei2*⁻ clone F2 were injected into 2 and 4 FRG NOD huHep mice, respectively. Mice were repopulated with human RBCs as depicted, and blood samples were removed for parasite 18S rRNA qRT-PCR on days 7 through 10. Blood samples from days 7 and 10 were transferred to in vitro culture for up to 10 days posttransition. (**B**) Schematic represents the experimental setup for results shown in Table 2 and in Supplemental Figure 8B. One million sporozoites from *P. falciparum* NF54 and *P. falciparum mei2*⁻ clones F2 and F5 were injected into 2, 2, and 4 FRG NOD huHep mice, respectively. Mice were repopulated with human RBCs as depicted, and 50 μL blood was collected from all mice for parasite 18S rRNA qRT-PCR samples on day 7. One mouse infected with *P. falciparum* NF54, 1 mouse infected with *P. falciparum mei2*⁻ clone F2, and 3 mice infected with *P. falciparum mei2*⁻ clone F5 were exsanguinated on day 7, and blood was transferred to in vitro culture. The remaining mice infected with each clone were sacrificed on day 8 and processed for 18S rRNA qRT-PCR and in vitro culture. All in vitro culture samples were maintained for up to 8 weeks.

studies to detect parasites in blood after challenge by 5–7 infectious mosquito bites (49–52). The assay has a detection limit of 20 parasite equivalents/mL (52). However, qRT-PCR for 18S rRNA can only provide information regarding the presence or absence of parasite nucleic acids. In vitro culture that enables expansion of parasitized RBCs is the most sensitive assay to detect the infectivity of released merozoites. For the mouse that had 1573 parasite equivalents/mL, at a very minimum multiplication rate of 2 per 24 hours, after 2 weeks in culture there should be 25 × $10^6$ parasites/mL of blood. This density of parasites is easily detectable by thick smear (49). However, the detected parasite 18S rRNA presumably did not originate from infectious exoerythrocytic merozoites that were culturable; i.e., we could not recover viable blood stage parasites by thick smears or detect parasites by qRT-PCR from blood transferred to in vitro culture even after prolonged culture. In contrast, when limiting dilution cloning was performed to derive clonal populations of blood stage *P. falciparum mei2*⁻, parasites were easily detected by thick smear between days 17 and 21 of culture (Supplemental Figure 8C), when parasites were seeded at an initial density of 3 parasites/mL. Moreover, all 14 clones retrieved were *P. falciparum mei2*⁻ and none were WT. Therefore, the inability to recover blood stage parasites after liver stage–to–blood stage transition is not due to impaired growth of *P. falciparum mei2*⁻ in the blood stage.

These results together demonstrate that *P. falciparum mei2*⁻ is severely attenuated late in liver stage development and cannot form or release infectious exoerythrocytic merozoites into the blood.

*Atypical extrusomes in P. falciparum mei2*⁻ *liver stages*. We further investigated the potential origin of parasite 18S rRNA that we had detected in the 2 of 10 FRG NOD huHep mice infected with *P. falciparum mei2*⁻ liver stages. We reasoned that nonviable *P. falciparum mei2*⁻ liver stages might release parasite material into the circulation, which resulted in the detection of parasite 18S rRNA by qRT-PCR. Previous studies using rodent malaria parasites have shown that merozoites are released from infected hepatocytes as extrusomes or

**Table 1. *P. falciparum mei2*⁻ liver stages do not transition to productive blood stage infection after sporozoite infection in FRG huHep mice repopulated with human RBCs and do not grow out in in vitro culture**

| Parasite strain[A] | Mouse | qRT-PCR for *P. falciparum* 18S rRNA from mouse blood on days 7, 8, 9, and 10 | In vitro culture from mouse blood collected on days 7 and 10[B] |
|---|---|---|---|
| *P. falciparum* NF54 | 1 | Detected | Detected |
| | 2 | Detected | Detected |
| *P. falciparum mei2*⁻ | 1 | Not detected | Not detected |
| | 2 | Not detected | Not detected |
| | 3 | Not detected | Not detected |
| | 4 | Detected on day 7 only | Not detected |

[A]Sporozoites from *P. falciparum mei2*⁻ clone F2 were used for the experiment. [B]Parasites were maintained in culture for 10 days.

merosomes (53–55). Extrusomes/merosomes were also reported to occur in *P. falciparum* liver stage–infected FRG huHep mice (43). These structures are clusters of dozens to hundreds of exoerythrocytic merozoites surrounded by hepatocyte plasma membrane that bud off from the infected hepatocyte into the sinusoidal lumen, travel to the lung, and are then released into the vasculature as infectious merozoites (53). We thus investigated the occurrence of these structures (herein referred to as extrusomes) further. We observed extrusomes in 5 of 14 randomly selected *P. falciparum* NF54 liver stages by IFA using a CSP antibody that delineates the PPM (Figure 9) at day 7 postinfection. Interestingly, we also detected extrusome-like structures associated with 15 of 23 randomly selected *P. falciparum mei2*⁻ liver stage schizonts at day 7 postinfection. It is possible that these extrusome-like structures released parasite material, albeit without infectious merozoites, into the vasculature. This might explain the detection of parasite 18S rRNA by qRT-PCR observed in *P. falciparum mei2*⁻–infected FRG huHep/FRG NOD huHep mice.

*Generation of P. falciparum mei2*⁻ *parasites free of extraneous DNA for potential human vaccination*. Our findings demonstrate that *P. falciparum mei2*⁻ parasites progress normally through the parasite life cycle and robustly form infectious sporozoites. However, after human hepatocyte infection, *P. falciparum mei2*⁻ parasites suffer a severe differentiation defect late in exoerythrocytic schizogony and cannot form infectious merozoites in the FRG huHep/FRG NOD huHep mouse models. These results encouraged us to prepare *P. falciparum mei2*⁻ parasites suitable for use as a live attenuated vaccine in humans. A whole-cell investigational product must be devoid of foreign DNA and should be susceptible to antimalarial drugs. Upon further analysis, we detected retention of the pFC-PlasMei2 plasmid in the *P. falciparum mei2*⁻ clones F2 and F5 by PCR for the plasmid component, Cas9 (Figure 10A). Whole-genome sequencing of genomic DNA isolated from *P. falciparum mei2*⁻ clone F2 revealed that the plasmid was retained episomally (data not shown). To generate *P. falciparum mei2*⁻ devoid of extraneous DNA, we modified the pFC plasmid to incorporate the negative selectable marker yeast cytosine deaminase/uridyl phosphoribosyl transferase (*yFCU*) (56). The truncated EF1α promoter in the pFC plasmid was replaced by the entire EF1α intergenic promoter region between the 2 EF1α genes, resulting in a bidirectional promoter that drove expression of the positive selectable marker, *hDHFR*, and the negative selectable marker, *yFCU* (Figure 10B and Supplemental Figure 1B). This plasmid, pFC-yFCU, was used to clone the *P. falciparum Mei2* donor repair templates and *P. falciparum Mei2*–specific guides to generate the pFC-PlasMei2-yFCU plasmid, which was transfected into *P. falciparum* NF54 parasites as previously described (33). Transfected parasites were screened for deletion of *P. falciparum Mei2* using PCR genotyping, followed by 2 rounds of negative selection using 5-fluorocytosine (5FC) to eliminate parasites that still retained the plasmid. No plasmid was detected by PCR after 2 rounds of 5FC treatment (Figure 10C). These parasites were cloned by limiting dilution; the clones were screened for lack of *Mei2* (Figure 10D) and lack of plasmid (Figure 10E) both by PCR genotyping and by whole-genome sequencing (data not shown). Marker-free clones were obtained from 2 independent transfections. Whole-genome sequencing of marker-free *P. falciparum mei2*⁻ clones confirmed that they were devoid of DNA from the pFC plasmid used for deletion and showed no apparent integration events within the parasite genome (data not shown). These clones are suitable for entering next steps in preclinical development, such as Master Cell Bank preparation under phase-appropriate good manufacturing practice conditions, which will allow the subsequent use of the *P. falciparum mei2*⁻ LARC GAP in human phase I clinical trials.

**Table 2. *P. falciparum mei2*⁻ liver stages from 2 independent clones do not transition to productive blood stage infection in FRG NOD huHep mice repopulated with human RBCs and do not grow out in long-term in vitro culture**

| Parasite strain | Mouse | qRT-PCR for *P. falciparum* 18S rRNA from mouse blood on days 7 and 8 | Long-term in vitro culture (8 weeks) |
|---|---|---|---|
| *P. falciparum* NF54 | 1 | Detected | Detected |
| | 2 | Detected | Detected |
| *P. falciparum mei2*⁻ F2 | 1 | Detected on day 7 only | Not detected |
| | 2 | Not detected | Not detected |
| *P. falciparum mei2*⁻ F5 | 1 | Not detected | Not detected |
| | 2 | Not detected | Not detected |
| | 3 | Not detected | Not detected |
| | 4 | Not detected | Not detected |

## Discussion

A vaccine for *P. falciparum* malaria that protects against liver infection and thereby prevents parasite life cycle progression to symptomatic blood stage infection and onward transmission by the mosquito vector has been an important goal for medicine and public health. Historically, the most studied live attenuated immunogen, *P. falciparum* RAS, which has been formulated for syringe immunization (24, 57) (PfSPZ), has proved to be a safe and highly efficacious vaccine in CHMI trials conducted in malaria-naive adults in the United States and Europe (20, 21, 58). Yet, PfSPZ did not confer complete protection when tested in Mali, an African country with high seasonal *P. falciparum* malaria transmission (21). Evidence suggests that persistent exposure to blood stage malaria infection can dysregulate immune responses and decrease vaccine efficacy (59). Indeed, Malian and Tanzanian adults had lower *P. falciparum* CSP antibody titers compared with malaria-naive US adults following PfSPZ vaccination (21, 59). This immune dysregulation could partly account for the limited efficacy of PfSPZ in malaria-exposed adult vaccinees and could be an obstacle to efficacy for other malaria vaccines.

Proof-of-concept human CHMI clinical trials with CPS by mosquito bite administration, followed more recently by syringe administration of fully infectious *P. falciparum* sporozoites with chloroquine prophylaxis (CVac), showed that improvements to whole-parasite vaccines are possible by allowing complete liver stage development of the whole-parasite immunogen. This generates durable sterilizing protection at a dose one-twentieth of that used with the PfSPZ vaccine (28, 29). Unfortunately, CVac carries a considerable safety liability; immunized individuals can potentially develop symptomatic if not lethal malaria blood stage infection through vaccination, if they fail to comply with the necessary drug regimen. Thus, the generation of an intrinsically attenuated *P. falciparum* parasite strain that infects the liver and undergoes substantial replication within hepatocytes but then ceases development and fails to form infectious exoerythrocytic merozoites is the ultimate goal of live attenuated malaria vaccine development efforts. Such LARC-attenuated parasites should not cause blood stage infection. Furthermore, LARC parasites should constitute superior immunogens because of their replication in the liver, which generates significant antigen biomass, a diverse antigenic repertoire for antigen presentation to T cells, and, at late liver stage, expression of blood stage antigens that might engender stage-transcending protection (26). Late liver stage attenuation can be achieved by genetic engineering of the parasite. Indeed proof-of-concept studies with *P. yoelii* rodent malaria LARC GAPs, lacking enzymes for type II fatty acid biosynthesis, (e.g., *P. yoelii fabb/f*⁻), demonstrated late liver stage arrest and superior protective efficacy in mice when compared with RAS and replication-deficient GAPs (60). Immunizations with *P. yoelii fabb/f*⁻ LARC GAP not only protected against homologous challenge in both inbred and outbred mice but also conferred protection against a sporozoite challenge using the different rodent malaria species *Plasmodium berghei* (species-transcending protection) and against lethal blood stage challenge of the same species (stage-transcending protection). The enhanced protection in *P. yoelii fabb/f*⁻ LARC GAP–immunized mice was attributed to cytotoxic $CD8^+$ T cells that recognized a broader repertoire of liver stage antigens (60). However, generating the equivalent LARC GAP in *P. falciparum* failed, as strains lacking enzymes for type II fatty acid biosynthesis did not generate sporozoites, indicating that this pathway is essential for *P. falciparum* sporozoite formation (37). The findings showed the limitations

**Table 3. Summary of attenuation of *P. falciparum mei2*⁻ preerythrocytic infection in FRG huHep/FRG NOD huHep mice**

| Parasite strain | No. of mice | qRT-PCR for *P. falciparum* 18S rRNA from mouse blood on day 7 | Thick smear positive in vitro culture |
|---|---|---|---|
| *P. falciparum* NF54 | 4 | 4/4 | 4/4 |
| *P. falciparum mei2*⁻ F2 | 6 | 2/6 | 0/6 |
| *P. falciparum mei2*⁻ F5 | 4 | 0/4 | 0/4 |

of rodent malaria models as predictors of stage-specific gene function in human malaria parasites, which is not surprising, considering the evolutionary divergence of *P. falciparum* and rodent malaria parasites (34, 35). Nevertheless, we recently reported that deletion of *Plasmodium Mei2* in *P. yoelii* resulted in a severe differentiation defect late during liver stage schizogony (38), and we have shown herein that deletion of *Mei2* in *P. falciparum* generated a convergent phenotype of late liver stage arrest. PlasMei2 proteins across all *Plasmodium* species are classified as putative RNA binding proteins because they have a highly conserved RNA recognition motif (RRM) that displays 96% identity and 98% similarity between *P. falciparum* and *P. yoelii* (38). This RRM is homologous to an RRM in Mei2-like proteins from other eukaryotes (61). Interaction of Mei2 with RNA has been shown only for the fission yeast *Schizosaccharomyces pombe* (*S. pombe*), in which it binds to the noncoding meiRNA (61–65). This Mei2-meiRNA complex is required for nuclear translocation of Mei2 and for exerting its functions in promoting DNA replication in the first meiotic division. Interestingly in plants, specifically in *Arabidopsis*, Mei2 was shown to be required for chromatin reorganization in meiosis; its absence resulted in formation of chromosomal abnormalities because of defects in DNA segregation (66, 67). These findings highlight that replication and segregation of DNA are 2 critical functions attributed to Mei2-like proteins from other eukaryotic species.

*Plasmodium* liver stage schizogony constitutes one of the most extensive cell growth and DNA replication events observed in eukaryotic cells. Liver stages replicate the single haploid parasite genome up to 50,000-fold and increase in cell volume up to 10,000-fold without undergoing cytokinesis (44). Then, at the end of schizogony this massive coenocyte undergoes cytokinesis and differentiates into tens of thousands of exoerythrocytic merozoites, each receiving a single genome as well as an apicoplast, mitochondria, and other essential organelles. Based on the clear homology of the PlasMei2 RRM with Mei2 proteins in other organisms (38, 61), it is reasonable to propose that this protein plays a critical role in liver stage DNA replication, chromatin reorganization, or cell division, a function wholly consistent with the liver stage

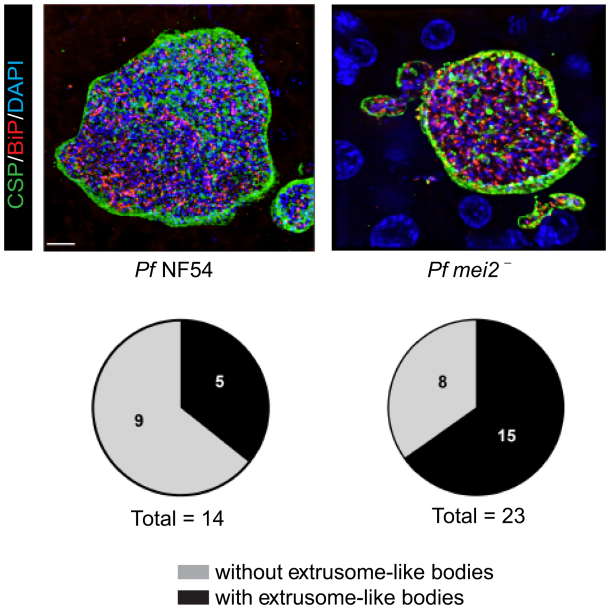


**Figure 9. Extrusome-like bodies were observed in *P. falciparum mei2*⁻ late liver stage schizonts.** Liver tissue sections from FRG NOD huHep mice infected with *P. falciparum* NF54 or *P. falciparum mei2*⁻ sporozoites were prepared on day 7 of liver stage development and used for IFA using antibodies against the PPM (CSP, green), ER (BiP, red), and DNA (DAPI). The pie chart shows the distribution of late liver stage schizonts with and without presence of extrusome-like bodies. Scale bar: 7 μm.

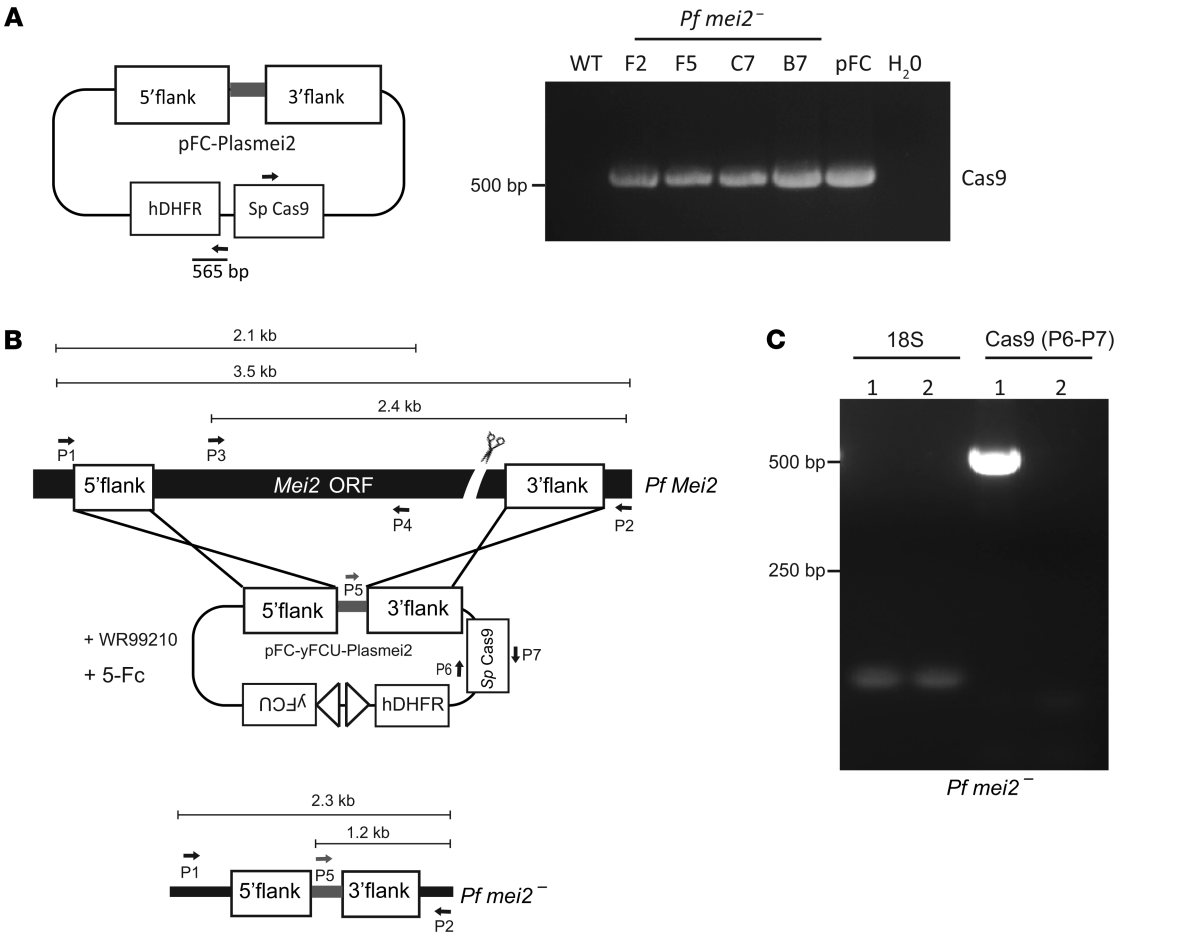


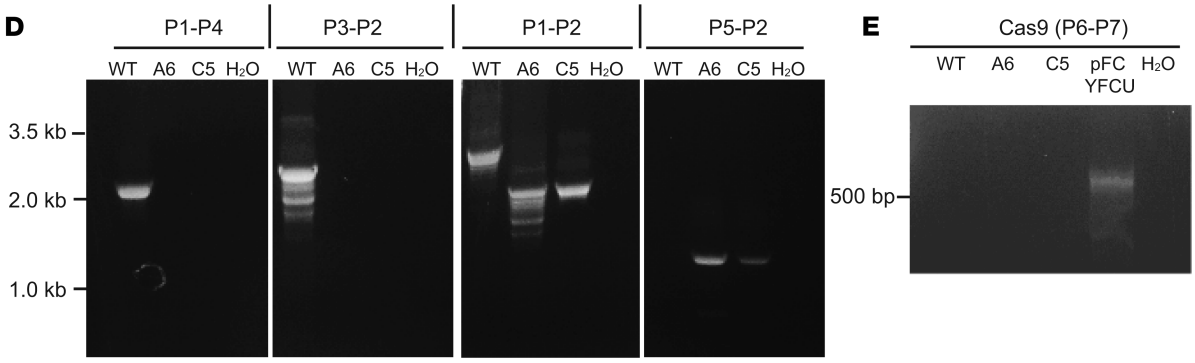


**Figure 10. Generation of marker-free *P. falciparum mei2*⁻.** (**A**) Cartoon showing the binding of primers specific for *S. pyogenes* Cas9 in the pFC-PlasMei2 plasmid. The PCR amplicon is 525 bp. Agarose gel electrophoresis shows the Cas9 PCR product amplified from genomic DNA of 4 *P. falciparum mei2*⁻ clones: F2, F5, C7, and B7. DNA from pFC-PlasMei2 was used as a positive control, and genomic DNA from *P. falciparum* NF54 was used as a negative control for the PCR. (**B**) The schematic depicts the generation of marker-free *P. falciparum mei2*⁻ using CRISPR/Cas9-mediated gene editing using the pFC-yFCU-PlasMei2 plasmid, carrying *yFCU* negative selection cassette. Primers used to verify gene deletion are indicated, and the sizes of the PCR products are shown below in kilobases. (**C**) Agarose gel electrophoresis shows the Cas9 PCR product amplified from genomic DNA of 2 independent transfections before limiting dilution cloning and before (column 1) and after (column 2) undergoing 2 rounds of negative selection. The Cas9 primers and the amplicon size are the same as in **A**. 18S rRNA was used as a positive control for the PCR reaction. (**D**) Agarose gel electrophoresis shows the PCR products corresponding to the gene deletion *P. falciparum mei2*⁻ clones A6 and C5 after positive and negative selection. PCR amplicons are shown in **B**. (**E**) Agarose gel electrophoresis shows absence of Cas9 PCR product amplified from genomic DNA of *P. falciparum mei2*⁻ clones A6 and C5, indicating no retention of plasmid. DNA from pFC-yFCU-PlasMei2 was used as a positive control, and genomic DNA from *P. falciparum* NF54 was used as a negative control for the PCR. The Cas9 primers and the amplicon size are the same as in **A**.

developmental defect described herein. Defective nuclear replication events would then result in downstream effects, such as defects in organelle replication, cytomere formation, and ultimately abrogation of merozoite formation, which we indeed observed in *P. falciparum mei2*$^-$ liver stages. Further characterization of PlasMei2 and its putative RNA binding partner will be important for understanding the biology of this essential liver stage protein.

Using the FRG and FRG NOD huHep mouse models additionally repopulated with human RBCs, we have shown here that *P. falciparum mei2*$^-$ parasites appear unable to form infectious exoerythrocytic merozoites and do not transition to a viable blood stage infection. It has been previously shown that challenge with only 5 *P. falciparum*–infected mosquito bites results in liver stage infection in these mice, and thus, the use of 1 million *P. falciparum mei2*$^-$ sporozoites used herein can be considered an extremely high challenge dose (68). None of the *P. falciparum mei2*$^-$ sporozoite-challenged humanized mice developed culturable asexual blood stage infection even after prolonged culture. Nonetheless, we detected parasite 18S rRNA in the blood of a few of the challenged mice using highly sensitive qRT-PCR. We speculate that this parasite nucleic acid is derived from nonviable extrusome-like bodies that we observed to be transiently released by *P. falciparum mei2*$^-$ late liver stage schizonts. It is possible that the cellular mechanisms involved in formation and release of such extrusomes are independent of full differentiation of the late liver stage schizont and exoerythrocytic merozoite formation.

Currently it remains unknown whether the FRG huHep model is sufficiently sensitive to fully mimic *P. falciparum* sporozoite infectivity in humans because direct quantitative comparisons are not possible. Thus, the residual blood stage breakthrough potential of *P. falciparum mei2*$^-$ parasites should be evaluated in a dose escalation CHMI trial in malaria-naive, adult human subjects. Three future paths for clinical development of a *P. falciparum* LARC GAP can be envisioned: (i) if CHMI trials show no breakthrough infection of *P. falciparum mei2*$^-$ at high sporozoites doses, this LARC GAP can be further developed as a standalone, next-generation, live-attenuated sporozoite vaccine. On the other hand, (ii) if low-frequency and low-grade breakthrough infections are observed in human subjects, *P. falciparum mei2*$^-$ can be subjected to additional gene deletions to achieve full liver stage attenuation, as we have shown with rodent malaria parasites (69). Last, (iii) *P. falciparum mei2*$^-$ sporozoites might be combined with chloroquine or another blood stage partner drug, and such a combination would reduce the risk in current CVac immunizations using fully infectious WT *P. falciparum*.

## Methods

Please refer to Supplemental Methods.

*Statistics*. Calculations and statistical tests indicated in the figure legends were performed using GraphPad Prism Software. The statistical tests used are 1-way and 2-way ANOVA and unpaired 2-tailed *t* test, as indicated. A *P* value less than 0.05 was considered significant.

*Study approval*. This study was carried out in accordance with the recommendations of the NIH Office of Laboratory Animal Welfare standards (welfare assurance D16-00119). Mice were maintained and bred under specific pathogen–free conditions at the Center for Global Infectious Disease Research, Seattle Children's Research Institute. The protocol was approved by the Center for Infectious Disease Research Institutional Animal Care and Use Committee under protocol 00480.

## Author contributions

SHIK, AMV, and DG conceived the work and designed experiments. DG, AMV, WB, NL, CP, CB, CS, NC, SYK, and TN carried out laboratory work and collected and analyzed data. WB, NC, and TN produced gametocytes and sporozoite-infected mosquitoes. CP and SCM created and analyzed the qRT-PCR data and contributed to discussion. DG, AMV, and SHIK wrote the manuscript.

## Acknowledgments

We thank the insectary team at the Center for Global Infectious Disease Research for providing *Anopheles stephensi* mosquitoes. We thank Donald Sodora and Chloe Jones for help with RNAscope technology. We thank the University of Washington Histology and Imaging Core for help with generating liver sections. We thank Ian Cheeseman for evaluating the genome sequences of NF54 and *P. falciparum mei2*$^-$ clones. This work was funded by the NIH (R01 AI125706).

Address correspondence to: Stefan H.I. Kappe, Center for Global Infectious Disease Research, Seattle Children's Research Institute, 307 Westlake Avenue N., Seattle, Washington 98101, USA. Phone: 206.884.3180; Email: Stefan.Kappe@seattlechildrens.org.

1. World Health Organization. World Malaria Report 2019. World Health Organization website. https://www.who.int/publications-detail/world-malaria-report-2019. Published December 4, 2019. Accessed June 4, 2020.
2. Moormann AM, Nixon CE, Forconi CS. Immune effector mechanisms in malaria: an update focusing on human immunity. *Parasite Immunol*. 2019;41(8):e12628.
3. Good MF, Doolan DL. Immune effector mechanisms in malaria. *Curr Opin Immunol*. 1999;11(4):412–419.
4. Crompton PD, et al. Malaria immunity in man and mosquito: insights into unsolved mysteries of a deadly infectious disease. *Annu Rev Immunol*. 2014;32:157–187.
5. Nahrendorf W, Scholzen A, Sauerwein RW, Langhorne J. Cross-stage immunity for malaria vaccine development. *Vaccine*. 2015;33(52):7513–7517.
6. Doolan DL, Dobaño C, Baird JK. Acquired immunity to malaria. *Clin Microbiol Rev*. 2009;22(1):13–36.
7. Lell B, et al. Impact of sickle cell trait and naturally acquired immunity on uncomplicated malaria after controlled human malaria infection in adults in Gabon. *Am J Trop Med Hyg*. 2018;98(2):508–515.
8. European Medicines Agency. First malaria vaccine receives positive scientific opinion from EMA. European Medicines Agency website. https://www.ema.europa.eu/en/news/first-malaria-vaccine-receives-positive-scientific-opinion-ema. Published July 24, 2015. Accessed June 4, 2020.
9. van den Berg M, Ogutu B, Sewankambo NK, Biller-Andorno N, Tanner M. RTS,S malaria vaccine pilot studies: addressing the human realities in large-scale clinical trials. *Trials*. 2019;20(1):316.
10. RTS,S Clinical Trials Partnership. Efficacy and safety of the RTS,S/AS01 malaria vaccine during 18 months after vaccination: a phase 3 randomized, controlled trial in children and young infants at 11 African sites. *PLoS Med*. 2014;11(7):e1001685.
11. Stoute JA, et al. A preliminary evaluation of a recombinant circumsporozoite protein vaccine against Plasmodium falciparum malaria. RTS,S Malaria Vaccine Evaluation Group. *N Engl J Med*. 1997;336(2):86–91.
12. Stoute JA, et al. Long-term efficacy and immune responses following immunization with the RTS,S malaria vaccine. *J Infect Dis*. 1998;178(4):1139–1144.
13. Bojang KA, et al. Efficacy of RTS,S/AS02 malaria vaccine against *Plasmodium falciparum* infection in semi-immune adult men in The Gambia: a randomised trial. *Lancet*. 2001;358(9297):1927–1934.
14. Alonso PL, et al. Duration of protection with RTS,S/AS02A malaria vaccine in prevention of *Plasmodium falciparum* disease in Mozambican children: single-blind extended follow-up of a randomised controlled trial. *Lancet*. 2005;366(9502):2012–2018.
15. Alonso PL, et al. Efficacy of the RTS,S/AS02A vaccine against *Plasmodium falciparum* infection and disease in young African children: randomised controlled trial. *Lancet*. 2004;364(9443):1411–1420.
16. Hoffman SL, et al. Protection of humans against malaria by immunization with radiation-attenuated *Plasmodium falciparum* sporozoites. *J Infect Dis*. 2002;185(8):1155–1164.
17. Hoffman SL, et al. Development of a metabolically active, non-replicating sporozoite vaccine to prevent *Plasmodium falciparum* malaria. *Hum Vaccin*. 2010;6(1):97–106.
18. Epstein JE, et al. Protection against *Plasmodium falciparum* malaria by PfSPZ Vaccine. *JCI Insight*. 2017;2(1):e89154.
19. Seder RA, et al. Protection against malaria by intravenous immunization with a nonreplicating sporozoite vaccine. *Science*. 2013;341(6152):1359–1365.
20. Lyke KE, et al. Attenuated PfSPZ Vaccine induces strain-transcending T cells and durable protection against heterologous controlled human malaria infection. *Proc Natl Acad Sci U S A*. 2017;114(10):2711–2716.
21. Sissoko MS, et al. Safety and efficacy of PfSPZ Vaccine against Plasmodium falciparum via direct venous inoculation in healthy malaria-exposed adults in Mali: a randomised, double-blind phase 1 trial. *Lancet Infect Dis*. 2017;17(5):498–509.
22. Nussenzweig RS, Vanderberg J, Most H, Orton C. Protective immunity produced by the injection of x-irradiated sporozoites of plasmodium berghei. *Nature*. 1967;216(5111):160–162.
23. Oakley MS, et al. Molecular markers of radiation induced attenuation in intrahepatic Plasmodium falciparum parasites. *PLoS One*. 2016;11(12):e0166814.
24. Epstein JE, et al. Live attenuated malaria vaccine designed to protect through hepatic $CD8^+$ T cell immunity. *Science*. 2011;334(6055):475–480.
25. Ishizuka AS, et al. Protection against malaria at 1 year and immune correlates following PfSPZ vaccination. *Nat Med*. 2016;22(6):614–623.
26. Goswami D, Minkah NK, Kappe SHI. Designer parasites: genetically engineered *Plasmodium* as vaccines to prevent malaria infection. *J Immunol*. 2019;202(1):20–28.
27. Vaughan AM, Kappe SHI. Genetically attenuated malaria parasites as vaccines. *Expert Rev Vaccines*. 2017;16(8):765–767.
28. Roestenberg M, et al. Long-term protection against malaria after experimental sporozoite inoculation: an open-label follow-up study. *Lancet*. 2011;377(9779):1770–1776.
29. Mordmüller B, et al. Sterile protection against human malaria by chemoattenuated PfSPZ vaccine. *Nature*. 2017;542(7642):445–449.
30. Kappe SH, et al. Exploring the transcriptome of the malaria sporozoite stage. *Proc Natl Acad Sci U S A*. 2001;98(17):9895–9900.
31. Matuschewski K, Ross J, Brown SM, Kaiser K, Nussenzweig V, Kappe SH. Infectivity-associated changes in the transcriptional repertoire of the malaria parasite sporozoite stage. *J Biol Chem*. 2002;277(44):41948–41953.
32. van Schaijk BC, et al. A genetically attenuated malaria vaccine candidate based on *P. falciparum* b9/slarp gene-deficient sporozoites. *Elife*. 2014;3:e03582.
33. Mikolajczak SA, et al. A next-generation genetically attenuated Plasmodium falciparum parasite created by triple gene deletion. *Mol Ther*. 2014;22(9):1707–1715.

34. Frech C, Chen N. Genome comparison of human and non-human malaria parasites reveals species subset-specific genes potentially linked to human disease. *PLoS Comput Biol*. 2011;7(12):e1002320.
35. Silva JC, Egan A, Friedman R, Munro JB, Carlton JM, Hughes AL. Genome sequences reveal divergence times of malaria parasite lineages. *Parasitology*. 2011;138(13):1737–1749.
36. Kublin JG, et al. Complete attenuation of genetically engineered Plasmodium falciparum sporozoites in human subjects. *Sci Transl Med*. 2017;9(371):eaad9099.
37. van Schaijk BC, et al. Type II fatty acid biosynthesis is essential for Plasmodium falciparum sporozoite development in the midgut of Anopheles mosquitoes. *Eukaryotic Cell*. 2014;13(5):550–559.
38. Dankwa DA, Davis MJ, Kappe SHI, Vaughan AM. A Plasmodium yoelii mei2-like RNA binding protein is essential for completion of liver stage schizogony. *Infect Immun*. 2016;84(5):1336–1345.
39. López-Barragán MJ, et al. Directional gene expression and antisense transcripts in sexual and asexual stages of Plasmodium falciparum. *BMC Genomics*. 2011;12:587.
40. Wang F, et al. RNAscope: a novel in situ RNA analysis platform for formalin-fixed, paraffin-embedded tissues. *J Mol Diagn*. 2012;14(1):22–29.
41. Azuma H, et al. Robust expansion of human hepatocytes in Fah-/-/Rag2-/-/Il2rg-/- mice. *Nat Biotechnol*. 2007;25(8):903–910.
42. Zhang C, et al. Efficient editing of malaria parasite genome using the CRISPR/Cas9 system. *mBio*. 2014;5(4):e01414–e01414.
43. Vaughan AM, et al. Complete *Plasmodium falciparum* liver-stage development in liver-chimeric mice. *J Clin Invest*. 2012;122(10):3618–3628.
44. Graewe S, Stanway RR, Rennenberg A, Heussler VT. Chronicle of a death foretold: Plasmodium liver stage parasites decide on the fate of the host cell. *FEMS Microbiol Rev*. 2012;36(1):111–130.
45. Stanway RR, et al. Organelle segregation into Plasmodium liver stage merozoites. *Cell Microbiol*. 2011;13(11):1768–1782.
46. Francia ME, Striepen B. Cell division in apicomplexan parasites. *Nat Rev Microbiol*. 2014;12(2):125–136.
47. Foquet L, et al. *Plasmodium falciparum* liver stage infection and transition to stable blood stage infection in liver-humanized and blood-humanized FRGN KO mice enables testing of blood stage inhibitory antibodies (reticulocyte-binding protein homolog 5) *in vivo*. *Front Immunol*. 2018;9:524.
48. Takenaka K, et al. Polymorphism in Sirpa modulates engraftment of human hematopoietic stem cells. *Nat Immunol*. 2007;8(12):1313–1323.
49. Murphy SC, et al. Real-time quantitative reverse transcription PCR for monitoring of blood-stage Plasmodium falciparum infections in malaria human challenge trials. *Am J Trop Med Hyg*. 2012;86(3):383–394.
50. Walther M, et al. Safety, immunogenicity and efficacy of a pre-erythrocytic malaria candidate vaccine, ICC-1132 formulated in Seppic ISA 720. *Vaccine*. 2005;23(7):857–864.
51. Hodgson SH, et al. Increased sample volume and use of quantitative reverse-transcription PCR can improve prediction of liver-to-blood inoculum size in controlled human malaria infection studies. *Malar J*. 2015;14:33.
52. Seilie AM, et al. Beyond blood smears: qualification of *Plasmodium* 18S rRNA as a biomarker for controlled human malaria infections. *Am J Trop Med Hyg*. 2019;100(6):1466–1476.
53. Sturm A, et al. Manipulation of host hepatocytes by the malaria parasite for delivery into liver sinusoids. *Science*. 2006;313(5791):1287–1290.
54. Baer K, Klotz C, Kappe SH, Schnieder T, Frevert U. Release of hepatic Plasmodium yoelii merozoites into the pulmonary microvasculature. *PLoS Pathog*. 2007;3(11):e171.
55. Tarun AS, et al. Quantitative isolation and in vivo imaging of malaria parasite liver stages. *Int J Parasitol*. 2006;36(12):1283–1293.
56. Mogollon CM, et al. Rapid generation of marker-free *P*. falciparum fluorescent reporter lines using modified CRISPR/Cas9 constructs and selection protocol. *PLoS One*. 2016;11(12):e0168362.
57. Hoffman SL, et al. Development of a metabolically active, non-replicating sporozoite vaccine to prevent Plasmodium falciparum malaria. *Hum Vaccin*. 2010;6(1):97–106.
58. Greenwood B. Progress with the PfSPZ Vaccine for malaria. *Lancet Infect Dis*. 2017;17(5):463–464.
59. Jongo SA, et al. Safety, Immunogenicity, and protective efficacy against controlled human malaria infection of *Plasmodium falciparum* sporozoite vaccine in Tanzanian adults. *Am J Trop Med Hyg*. 2018;99(2):338–349.
60. Butler NS, Schmidt NW, Vaughan AM, Aly AS, Kappe SH, Harty JT. Superior antimalarial immunity after vaccination with late liver stage-arresting genetically attenuated parasites. *Cell Host Microbe*. 2011;9(6):451–462.
61. Jeffares DC, Phillips MJ, Moore S, Veit B. A description of the Mei2-like protein family; structure, phylogenetic distribution and biological context. *Dev Genes Evol*. 2004;214(3):149–158.
62. Watanabe Y, Lino Y, Furuhata K, Shimoda C, Yamamoto M. The S.pombe mei2 gene encoding a crucial molecule for commitment to meiosis is under the regulation of cAMP. *EMBO J*. 1988;7(3):761–767.
63. Watanabe Y, Yamamoto M. S. pombe mei2+ encodes an RNA-binding protein essential for premeiotic DNA synthesis and meiosis I, which cooperates with a novel RNA species meiRNA. *Cell*. 1994;78(3):487–498.
64. Watanabe Y, Shinozaki-Yabana S, Chikashige Y, Hiraoka Y, Yamamoto M. Phosphorylation of RNA-binding protein controls cell cycle switch from mitotic to meiotic in fission yeast. *Nature*. 1997;386(6621):187–190.
65. Yamashita A, Watanabe Y, Nukina N, Yamamoto M. RNA-assisted nuclear transport of the meiotic regulator Mei2p in fission yeast. *Cell*. 1998;95(1):115–123.
66. Anderson GH, Hanson MR. The Arabidopsis Mei2 homologue AML1 binds AtRaptor1B, the plant homologue of a major regulator of eukaryotic cell growth. *BMC Plant Biol*. 2005;5:2.
67. Kaur J, Sebastian J, Siddiqi I. The Arabidopsis-mei2-like genes play a role in meiosis and vegetative growth in Arabidopsis. *Plant Cell*. 2006;18(3):545–559.
68. Sack BK, et al. Humoral protection against mosquito bite-transmitted *Plasmodium falciparum* infection in humanized mice. *NPJ Vaccines*. 2017;2:27.
69. Vaughan AM, et al. A *Plasmodium* parasite with complete late liver stage arrest protects against preerythrocytic and erythrocytic stage infection in mice. *Infect Immun*. 2018;86(5):e00088-18.